Asian Journal of Chemistry; Vol. 27, No. 7 (2015), 2548-2554

ASIAN JOURNAL OF CHEMISTRY

http://dx.doi.org/10.14233/ajchem.2015.18229

Morphology and Mechanical Properties of Poly(trimethylene terephthalate)/Maleinized Acrylonitrile-Butadiene-Styrene Blends

YUQING BAI, NA LI, YINGBIN LIU and MINGTAO RUN*

College of Chemistry and Environmental Science, Hebei University, Baoding 071002, Hebei Province, P.R. China

*Corresponding author: Fax: +86 312 5079525; E-mail: lhbx@hbu.edu.cn

Received: 31 May 2014; *Accepted*: 12 August 2014; *Published online*: 30 March 2015; AJC-17077

Poly(trimethylene terephthalate) was melt-blended with maleinized acrylonitrile-butadiene-styrene to enhance its toughness without sacrificing comprehensive performance. The advantage of using acrylonitrile-butadiene-styrene-g-maleinized blends (ABS-g-MAH) is due to its high toughness, good processing properties and higher molecular polarity. The phase morphology, mechanical properties, crystallization behaviors, dynamic mechanical behaviors, rheology, spherulites morphology, thermal stability and thermal aging properties were investigated by scanning electron microscopy, universal tester, differential scanning calorimetry, dynamic mechanical analyzer, capillary rheometer, polarized optical microscopy, thermogravimetric analyzer and color-difference meter, respectively. The results suggest that the dimension of the dispersed phase is lower than 1 mm and the interface between acrylonitrile-butadiene-styrene and poly(trimethylene terephthalate) is not sharp. Therefore, acrylonitrile-butadiene-styrene is compatible with poly(trimethylene terephthalate) (PTT). With addition of 5 % acrylonitrile-butadiene-styrene, the yielding strength, breaking strength and impact strength of the blends increase 41.5, 167 and 200 % than those of pure poly(trimethylene terephthalate); therefore, acrylonitrile-butadiene-styrene can not only greatly toughen poly(trimethylene terephthalate) but also reinforce poly(trimethylene terephthalate) to some extent with proper additions. Acrylonitrile-butadiene-styrene also serves as a nucleating agent for increasing the crystallization rate. The blends show larger storage modulus and higher glass transition temperatures than those of pure poly(trimethylene terephthalate). Acrylonitrile-butadiene-styrene improves the processing property of poly(trimethylene terephthalate) by increasing the apparent viscosity of the blends. However, the blends of PTT/ABS show decreased thermal aging resistance of the blends.

Keywords: Poly(trimethylene terephthalate), Mechanical properites, Compatibility, Thermal aging property, Polymer blends and alloys.

INTRODUCTION

Poly(trimethylene terephthalate) (PTT) is a linear aromatic polyester which was first produced by Shell Chemicals under the trade name Corterra®[1]. As an engineering thermoplastic, it combines good mechanical properties like poly(ethylene terephthalate) and good processing properties like poly(butylene terephthalate) into one polymer[2,3]. However, poly(trimethylene terephthalate) has some shortcomings, such as low heat-distortion temperature, low impact strength at low temperature and low viscosity for processing.

Polymer blending is a straightforward, versatile and inexpensive method for obtaining new materials with better properties[4,5]. The important studies on blends of poly(trimethylene terephthalate) with other polymer include poly(trimethylene terephthalate) and PEN[6,7], poly(trimethylene terephthalate) and poly(butylene terephthalate)[8], poly(trimethylene terephthalate) and poly(ethylene terephthalate)[9], poly(trimethylene terephthalate) and EPDM[10,11], poly(trimethylene terephthalate) and acrylonitrile-butadiene-styrene[12], poly(trimethylene terephthalate) and PS[13], poly(trimethylene terephthalate) and metallocene LLDPE[14], poly(trimethylene terephthalate) and polypropylene[15,16], poly(trimethylene terephthalate), poly(butylene terephthalate) and poly(ethylene terephthalate)[17], poly(trimethylene terephthalate), EPDM and metallocene PE[18], *etc*. These blends have some improved properties, such as crystallization, mechanical and rheological properties. In general, the physical, mechanical and rheological properties of immiscible polymer blends depend not only on the constituent polymers but also on the morphologies of the blends. As is well-known, most of these blends are immiscible and incompatible. Some compatibilizers have been used, these include epoxy[12,19], EMP-MA[11] and styrene-butadiene-maleic anhydride[12], *etc*. Xue *et al.*[12] prepared PTT/ABS blends by melt processing with or without epoxy or styrene-butadiene-maleic anhydride copolymer as a reactive compatibilizer. They found that poly(trimethylene terephthalate) is partially miscible with acrylonitrile-butadiene-styrene over the entire composition range and both the compatibilizers have compatibilization effects on the blends. As an extensively commercial polymer,

acrylonitrile-butadiene-styrene is associated with good processability, dimensional stability and high impact strength at low temperatures[20-22]. Acrylonitrile-butadiene-styrene is a feasible choice for blending with poly(trimethylene terephthalate). In order to improve the miscibility of the polymer matrix with acrylonitrile-butadiene-styrene, some maleinized acrylonitrile-butadiene-styrene copolymers are usually used as compatibilizers[23].

In this work, poly(trimethylene terephthalate) was melt-blended with the maleinized acrylonitrile-butadiene-styrene (ABS-*g*-MAH) for improving its toughness, crystallization and rheological properties. Then the influences of ABS-*g*-MAH concentrations on the phase morphology, mechanical and thermal properties of the blends were also investigated.

EXPERIMENTAL

Raw materials: Poly(trimethylene terephthalate) homopolymer was supplied in pellet form by Shell Chemicals (USA) with an intrinsic viscosity of 0.90 dL/g measured in a phenol/tetrachloroethane solution (50/50, w/w) at 25 °C. The ABS-*g*-MAH used in our experiment was supplied by Shenyang Siwei Co. Ltd. (China) in pellet form with a density of 1.03 g/cm^3, MFR ≥ 7 g/min (2160 g, 190 °C) and a grafting ratio of 7-9 %.

Blends preparation: Poly(trimethylene terephthalate) and ABS-*g*-MAH were dried in a vacuum oven at 80 and 60 °C, respectively for 24 h before preparing the blends. Poly(trimethylene terephthalate) and ABS-*g*-MAH were mixed together with different weight ratios of ABS-*g*-MAH/PTT as follows: B0: 0/100; B1: 1/99; B2: 2/98; B3: 3/97; B4: 4/96; B5: 5/95; B7.5: 7.5/92.5; B10: 10/90; B100: 100/0 and then melt-blended in a SHJ-20 type, self-wiping, co-rotating twin-screw extruder (Nanjing Giant Machinery Co., China) operating at a screw speed of 100 rpm and with temperatures of 210, 235, 250, 255, 255, 250 °C from the first section to the die. The resultant blend ribbons were cooled in cold water, cut up and re-dried before being used in measurements.

Morphology: The morphology of the fracture surface, coated with a thin layer of gold, was observed by a KYKY-2800B type scanning electron microscopy (KYKY Technology Development Ltd., China) at an acceleration voltage of 25 kV. The fracture surfaces were made by impacting the cold blend ribbons in liquid nitrogen.

The spherulites morphology was performed on the polarized optical microscopy (BX-51, Olympus, Japan) with a digital camera system. Samples were pressed between two glass slides with a separation of about 100 μm after first melting on a hot stage at 240 °C for 10 min; they were then cooled to room temperature at a cooling rate of 1 °C/min, with the photographs taken at room temperature.

Differential scanning calorimetry: The melt-crystallization behaviors measurements of various blends were performed on a Diamond differential scanning calorimetry instrument (Perkin-Elmer Co., USA), which was calibrated with indium prior to use; the weights of the samples were approximately 7 mg. The as-extruded samples were heated to 260 °C at 80 °C/min under nitrogen atmosphere, held for 5 min, then cooled to 0 °C at a constant cooling rate of 10 °C/min, and the cooling process was recorded.

Mechanical properties: Pure poly(trimethylene terephthalate) and the blends were prepared into the sheets with the size of 100 mm × 100 mm × 3.6 mm by a compression molding method at 250 °C; then the sheets were cut into the special splines used in different measurements by a milling machine. The tensile testing method was done according to the ASTM D638 on a Universal Testing Machine (WSM-20, Changchun Intelligent Instrument & Equipment Co. Ltd, China) at room temperature, using the cross-head speed of 10 mm/min. The unnotched Charpy impact tests were carried out according to the ISO 179-1982 standard using splines with size of 60 mm × 6 mm × 4 mm and an impact tester (JJ-20, Changchun Intelligent Instrument Co. Ltd., China). All the above data reported were the mean and standard deviation from five determinations.

Fourier transform infrared spectroscopy (FTIR) characterization: FTIR spectra were recorded with a Varian-640 spectrophotometer (KBr pellet technique) in the wavenumber from 4000 to 500 cm^{-1} with a resolution of 1 cm^{-1} and averaged over 40 scans.

Rheological performance: The rheological measurements were performed on a XLY-II type capillary rheometer (Jilin University, China) at the temperature range from 230 to 260 °C. The capillary length and diameter are 40 and 1 mm, respectively. The sample of about 1.5 g was put into the capillary at fixed temperature, held for 10 min and then measured at the shear stress range of 12-240 kPa. Melt apparent viscosities are calculated by the Hagen-Poiseuille equation[24].

Thermal stability: The decomposition behaviors of the composites were measured on a Pyris 6 type thermogravimetric analyzer (TGA, Perkin-Elmer Co., USA) in the temperature range of 30-700 °C under nitrogen atmosphere at a heating rate of 20 °C/min.

The thermal aging properties of the blends were tested in an oven at 150 °C for 0-20 h aging times. The yellow index (Yid), white index (Wr) and color difference (ΔE) were measured on an auto color-difference meter (SC-800C, Beijing Kang-guang Co., China).

Dynamic mechanical characterization: The dynamic mechanical properties of the blends were performed on a dynamic mechanical analyzer (DMA, DMA8000, Perkin-Elmer Co., USA) using a single-cantilever vibration mode in the temperature range of 0-170 °C at a constant heating rate of 2 °C/min and a frequency of 2 Hz. The standard splines with the size of 10 × 5 × 2 mm were made by compression molding method at 250 °C.

RESULTS AND DISCUSSION

Phase morphology: Fig. 1 shows the SEM images of fracture surfaces of different samples. It can be seen in Fig. 1a, the fracture surface is not smooth and many strips were observed on the fracture surface, so it is concluded that poly(trimethylene terephthalate) underwent ductile fracture at low temperatures (< –100 °C); however, these strips were parallel to each other (parallel to the impact direction) but not regular in the direction, so poly(trimethylene terephthalate) has somewhat brittleness at low temperatures (< –100 °C). In Fig. 1b, the blend with 2 % ABS-*g*-MAH shows a different morphology, in which the surface becomes much rougher and only a few parallel rucks

can be observed, indicating that the blend absorbs more energy in breaking than that occurred in pure poly(trimethylene terephthalate). In Fig. 1c, the blend with 5 % ABS-*g*-MAH shows no parallel rucks on the rough surface. As shown in Fig. 1d and e , although the surfaces are rough, they become more and more planar with ABS-*g*-MAH contents increasing from 7.5 to 10 %. As the magnification is 500, no dispersed ABS-*g*-MAH phase can be observed clearly in the image (b-e); while as the magnification is 6,000, the ABS-*g*-MAH phases are finely dispersed in the matrix with the size lower than 1 mm in Fig. 1f and the ABS-*g*-MAH phases do not form sharp boundaries with the matrices. These results suggest that they have some phase interactions.

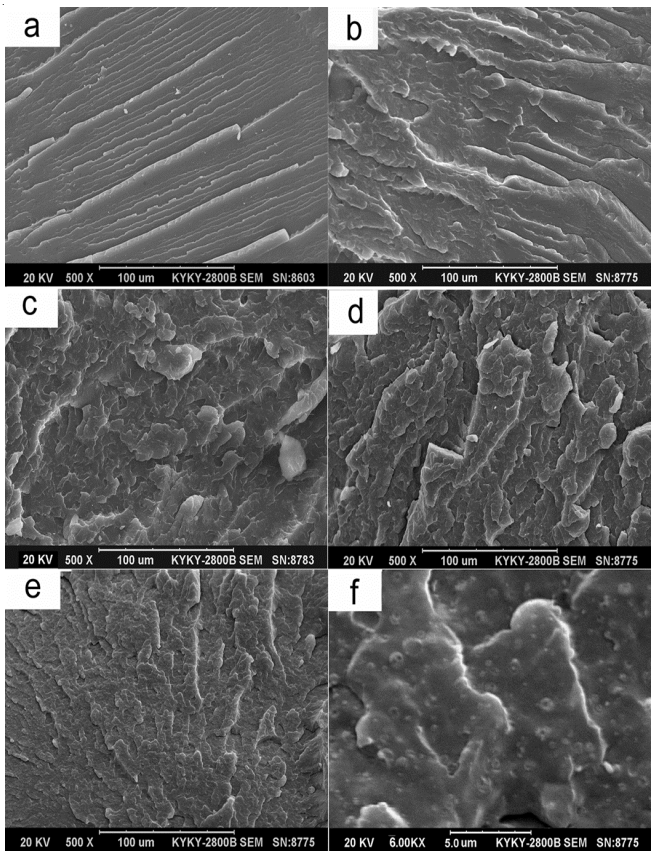

Fig. 1. SEM micrographs of the fracture surface of different PTT/ABS-*g*-MAH blends; (a) B0 × 500; (b) B2 × 500; (c) B5 × 500; (d) B7.5 × 500; and (e) B10 × 500; (f) B10 × 6000

As we known, if chemical reactions occurred between two polymers in the melt-blending processing, a copolymer may be formed *in situ* and acted as a compatibilizer. As shown in **Scheme-I**, when the poly(trimethylene terephthalate) and ABS-*g*-MAH were melt blended at 240-255 °C, the ABS-*g*-MAH having maleic anhydride group was expected to react with the hydroxyl end group of poly(trimethylene terephthalate) to form a graft copolymer (PTT-*g*-ABS) at the blend interface. As a result, the copolymer PTT-*g*-ABS can be a compatibilizer for poly(trimethylene terephthalate) and ABS-*g*-MAH. Similar reactions of hydroxyl group of polyester with anhydrides have been reported[25,26]. However, this reaction is reversible and its equilibrium is highly shifted to the reactant side with increasing temperature[27]. A temperature as high as 255 °C certainly

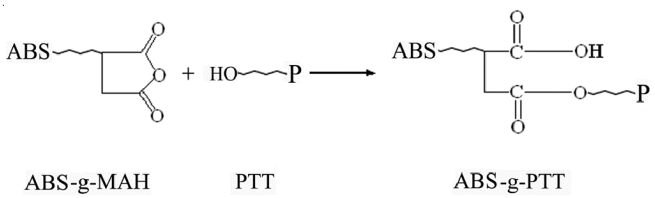

Scheme-I: Polycondensation reaction between hydroxyl end group of poly(trimethylene terephthalate) and maleic group of ABS-*g*-MAH leading to the formation of graft copolymer

corresponds to an equilibrium which is unfavorable for the formation of the PTT-*g*-ABS. In order to verify whether the graft copolymer is formed in the blends, the FTIR spectra of the blends were characterized and the spectra of poly(trimethylene terephthalate), ABS-*g*-MAH and PTT/ABS10 % blend were shown in Fig. 2. As seen in Fig. 2, the absorption bands of ABS-*g*-MAH at 1866-1862 cm^{-1} (asymmetric C=O stretching in MAH) and 1782 cm^{-1} (symmetric C=O stretching in MAH) were also observed in the spectra of PTT/ABS10 % blend. From the FTIR spectra, it is not sure whether or how many grafted polyesters had formed in the blend. Therefore, FTIR spectroscopy is not successful in identifying the nature of these interactions due to the complexity of the spectra and the overlapping of most of the characteristic peaks.

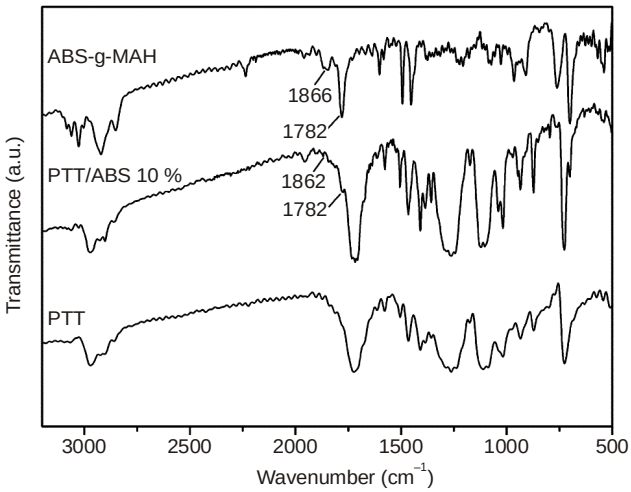

Fig. 2. FTIR spectra of ABS-*g*-MAH, PTT/ABS10 % and poly(trimethylene terephthalate)

However, it is also expected that the intermolecular dipole-dipole interactions and interchange reactions between OH, -COOH and ester groups in the case of maleic anhydride modified polymers and polyesters. If it occurs in the blends, the formed graft copolymer will reduce the interfacial tension and suppress the coalescence behaviour. In addition, the presence of the graft copolymer at the blend interface will broaden the interfacial region through the penetration of the copolymer chain segments into the corresponding adjacent phases[28]. On the other hand, the ABS-*g*-MAH has larger polarity than ungrafted acrylonitrile-butadiene-styrene. Therefore, the anhydride group in ABS-*g*-MAH will produce a more polar phase capable of enhanced interactions with the poly(ethylene terephthalate) phase.

Mechanical properties: It is known that the toughening effect of rubber particles depends on their size, distribution

and particle/matrix interaction[29,30]. These phase-separated particles, especially after the cavitation process, induce large stress concentrations which lead to extensive shear deformation with a high-energy absorbing mechanism[31,32]. Thus, it can be deduced that the mechanical properties of the blends will be better from the small size and uniform distribution of ABS-*g*-MAH and the strong ABS-*g*-MAH/PTT interface adhesion.

The mechanical properties were listed in Table-1. Pure PTT(B0) has the smallest yield strength, break strength and unnotched impact strength although it has the largest elongation at breaking point among these samples. The blends have larger yield strength, break strength and unnotched impact strength than those of pure poly(trimethylene terephthalate). B4 blend has the largest yield strength, break strength and tensile modulus; while the B5 blend has the largest unnotched impact strength, which is nearly 3 times than that of pure poly(trimethylene terephthalate). The above results suggest that 5 % ABS-*g*-MAH can apparently toughen poly(trimethylene terephthalate) as well as reinforce poly(trimethylene terephthalate). This may be related to three reasons: (1) the hard chain segments in ABS-*g*-MAH molecules, the acrylonitrile and the styrene chain segments, have larger strength which will reinforce poly(trimethylene terephthalate); (2) the soft chain segments in ABS-*g*-MAH molecules (such as the butadiene chain segments) which have larger impact strength can toughen poly(trimethylene terephthalate); (3) the smaller size spherulites in the blends will also be favorable for improving the impact strength of poly(trimethylene terephthalate), as shown in the following Fig. 3. Of course, it is believed that these mechanical results are attributed to the counterbalance of above effects. It can be safely assumed from the above morphological and mechanical properties that poly(trimethylene terephthalate) will be compatible with ABS-*g*-MAH.

TABLE-1
MECHANICAL PROPERTIES OF
DIFFERENT PTT/ABS-*g*-MAH BLENDS

Sample	σ_y [a] (MPa)	σ_b [b](MPa)	ε[c] (%)	E[d] (MPa)	σ_i [e] (kJ/m^2)
B0	31.3	15.8	289	1462	16.7
B1	37.5	35.9	17.3	1444	25.4
B2	41.3	39.5	14.9	1101	27.7
B3	41.2	39.4	14.7	1186	30.0
B4	44.4	42.9	14.9	990	41.1
B5	44.3	42.2	16.8	1086	50.2
B7.5	41.1	40.3	16.5	1129	40.9
B10	42.2	41.3	12.8	1047	29.5
ABS	44.2	39.4	12.3	1307	73.2

[a]Yield strength; [b]Break strength; [c]Elongation at breaking point; [d]Tensile modulous; [e]Unnotched impact strength

Spherulites morphology and melt-crystallization behaviours: Fig. 3 shows the spherulites morphology of different samples. In Fig. 3a, several large Maltese cross extinctions are observed obviously in pure poly(trimethylene terephthalate) and the spherulites are much larger and more perfect than the others shown in the blends of B2, B5 and B10. As shown in Fig. 3b-d, with increasing ABS-*g*-MAH content, the spherulites morphology changes significantly, *i.e.*, the spherulites dimensions become smaller and smaller and the perfection becomes worse and worse. For B2, the spherulites dimension is relatively

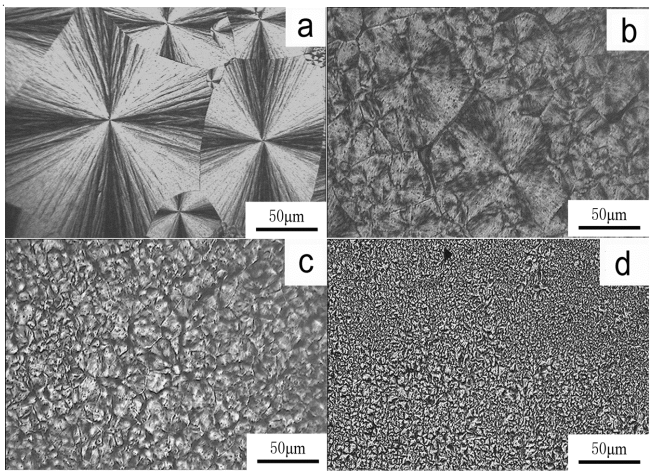

Fig. 3. Polarized optical microscopy images of different PTT/ABS-*g*-MAH blends; (a) B0, (b) B2, (c) B5, (d) B10

large and the Maltese cross extinction is observed obviously. For B5, the spherulites dimension is significantly reduced and the maltese cross extinction becomes weak. For B10, the spherulites dimension is smallest and no clear Maltese cross extinctions can be observed because the spherulites are more disordered and distorted.

The melt-crystallization behaviors are usually influenced by the addition of another polymer. Fig. 4 shows the differential scanning calorimetry cooling curves of eight samples with various ABS-*g*-MAH contents at the cooling rate of 10 °C/min; the resulting parameters are listed in Table-2. According to Fig. 4 and Table-2, the crystallization peak temperature (T_{cp}) of neat poly(trimethylene terephthalate) was the lowest of all samples and the T_{cp} of the blends shifted to higher temperature with increasing ABS-*g*-MAH content from 1 to 5 %. However, when ABS-*g*-MAH content increases from 5 to 10 %, the T_{cp} values remained unchanged. Moreover, the full width at half-height of the crystallization peak (FWHP) decreases as ABS-*g*-MAH content increased; especially when ABS-*g*-MAH contents are 7.5 and 10 %, the FWHP was only 2.8 °C. The crystallization enthalpy (ΔH_c) of pure PTT(B0) was the largest among all the samples. The above phenomena in Figs. 3 and 4 suggest two conclusions: (1) ABS-*g*-MAH served as a nucleating agent for poly(trimethylene terephthalate) crystallization due to its hard segments in the molecules, such as the acrylonitrile and the styrene segments (SAN); thus it increased both the initial crystallization temperature and the crystallization rate of poly(trimethylene terephthalate). The crystallization of different blends (B1-B10) was a nucleation controlled process and the nuclei in blends may be more active than those in PTT(B0), so the crystal growth process was depressed and the ΔH_c decreased with increasing ABS-*g*-MAH content; (2) when ABS-*g*-MAH content was increased to above 5 %, its effect of promoting the crystallization reached saturation.

Dynamic mechanical properties: The dynamic mechanical behaviours of different blends were investigated from 0 °C up to 170 °C and dynamic mechanical analyzer curves are presented in Figs. 5 and 6. Fig. 5 shows the relationship between the storage moduli (E′) with the temperature. In the temperature range of 0-50 °C, it can be seen that E′ is changed with different ABS-*g*-MAH content, *i.e.*, pure ABS-*g*-MAH

TABLE-2
CRYSTALLIZATION PARAMETERSFOR
PTT/ABS-*g*-MAH Blends

Sample	T_{cp}(°C)	ΔH_c[a](J/g)	FWHP (°C)
B0	180.1	-56.8	5.6
B1	185.9	-48.2	4.0
B2	188.6	-46.5	3.8
B3	190.6	-46.6	3.6
B4	191.5	-47.8	4.0
B5	194.9	-45.6	3.8
B7.5	194.6	-48.2	2.8
B10	194.3	-47.8	2.8

[a]Enthalpy has been normalized for poly(trimethylene terephthalate) contents

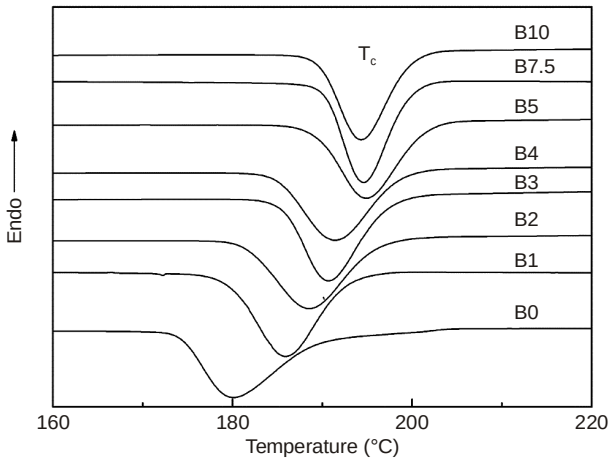

Fig. 4. Crystallization differential scanning calorimetry curves of the different blends

has the lowest modulus among all the samples; poly(trimethylene terephthalate) has a higher storage modulus than that of pure ABS-*g*-MAH. The storage modulus of all the blends are higher than those of pure poly(trimethylene terephthalate) and pure ABS-*g*-MAH and the blend with 3 % ABS-*g*-MAH has the highest one. These results suggest that ABS-*g*-MAH has a reinforcement effect on poly(trimethylene terephthalate).

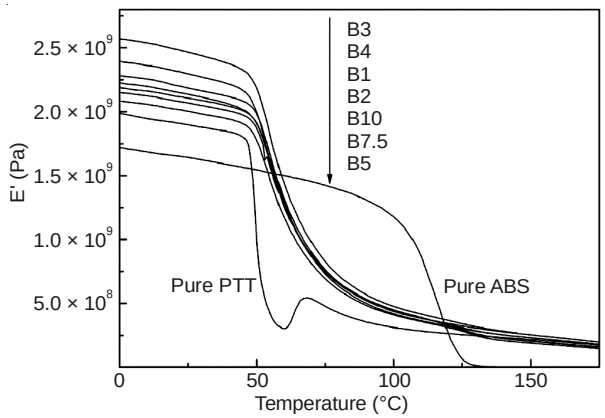

Fig. 5. Curves of storage modulus vs. temperature for different blends

In the temperature range of 50-160 °C, the storage modulus of poly(trimethylene terephthalate) and ABS-*g*-MAH decreases sharply at around 50 and 125 °C; while the storage modulus of the blends decreases slowly with increasing temperature. The slowly decreased modulus of the blends indicates that the hard chain segments of ABS-*g*-MAH (SAN) greatly impede the movement of poly(trimethylene terephthalate) chain segments. It can be found that this impeding effect is apparent with even only 1 % ABS-*g*-MAH in the blend. Thus, it can be concluded that there are strong interface interactions between poly(trimethylene terephthalate) phase and ABS-*g*-MAH phase and the chain segments' motions of poly(trimethylene terephthalate) are hindered by these interactions. At around 125 °C, a small decrease of the modulus can also be observed, especially for the blends with more ABS-*g*-MAH content, which corresponds to the glass transition of ABS-*g*-MAH component. When the temperature rises above 70 °C, the E′ increases with increasing temperature due to the cold-crystallization of poly(trimethylene terephthalate) molecules; however, no cold-crystallization behaviors can be observed in the blends.

The glass transition of these samples can also be seen in Fig. 6, which shows the curves of tan δ *vs.* temperature. From the results, pure poly(trimethylene terephthalate) and pure ABS-*g*-MAH have sharp tand peaks at 52.7 and 129.8 °C respectively. While for different blends, each has two separated weak tand peaks at around 69 °C (T_{g1}) and 126 °C (T_{g2}), corresponding to the glass transition of poly(trimethylene terephthalate) phase and the SAN of ABS-*g*-MAH phase in the blends respectively. This result indicates that poly(trimethylene terephthalate) and ABS-*g*-MAH are compatible in the blend because of their changes on the T_gs values. Even in the blend of B1 that only has 1 % ABS-*g*-MAH, its glass transition peak intensity at about 69 °C decreased greatly; this result clearly show the influence of ABS-*g*-MAH component on the mobility of the poly(trimethylene terephthalate) molecular chain segments. It can be seen that the tan δ peaks of ABS-*g*-MAH phase become larger with increasing ABS-*g*-MAH content.

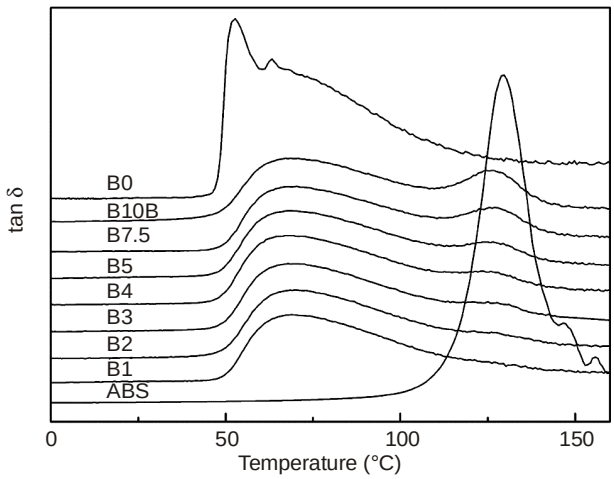

Fig. 6 Curves of tan δ *vs.* temperature for different blends

Rheological behaviours: Fig. 7 shows the rheological curves of different melts at 240 °C in the form of the plot of apparent viscosity *vs.* shearing rate. The results show that all the melts are pseudo-plastic fluids for the apparent viscosity decreases greatly with increasing shear rate. The pure ABS-*g*-MAH has the largest apparent viscosity and the strongest sensitivity to shearing rate among all the samples in low shearing rates and its apparent viscosity is lower than those of the bends as shearing rate is larger than 450 s^{-1} due to the

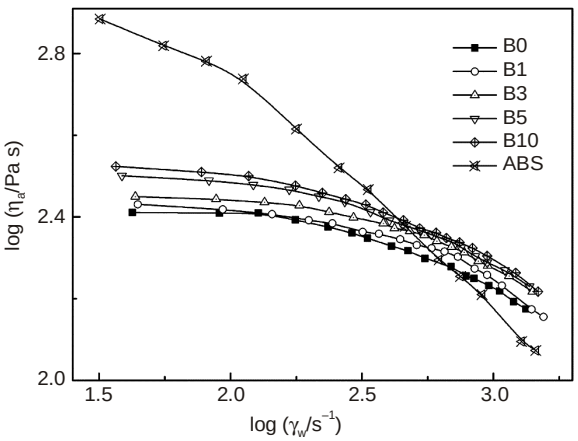

Fig. 7. Plots of log η_a *vs*. log γ_w

unentanglement of the molecules. For each blend, their apparent viscosity decreases slowly with increasing shearing rate; while the blends' apparent viscosity increases with increasing ABS-*g*-MAH contents. Therefore, the increasing viscosity may be favorable for improving the processing property of poly(trimethylene terephthalate) by adding more than 5 % ABS-*g*-MAH.

The Non-Newtonian index was calculated and its relationship with ABS-*g*-MAH content is shown in Fig. 8. It is observed that n is less than 1 for their pseudo-plastic fluid behaviors and it decreased with increasing ABS-*g*-MAH content. This result suggests that the pseudoplasticity is increased slightly with increasing ABS-*g*-MAH content.

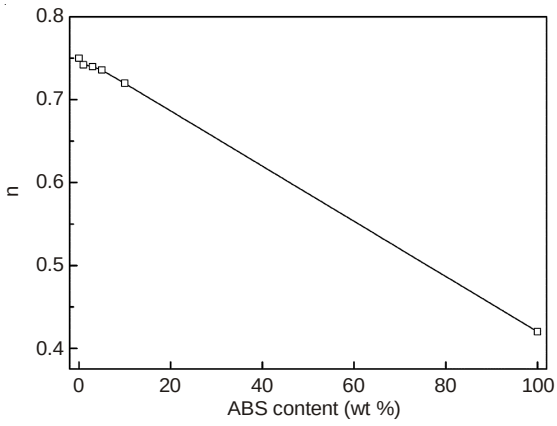

Fig. 8. Relationship between n and ABS-*g*-MAH contents

At different temperatures, the melt apparent viscosity *vs.* ABS-*g*-MAH content was plotted in Fig. 9. It is clear that the melt viscosity increases with increasing ABS-*g*-MAH content at the same temperature, while it decreases greatly with increasing temperatures from 230 to 260 °C, indicating that the temperature has large influence on the viscosity and it will influence the material processing. The Andrade-Arrhenius equation[33] can be used to illustrate the dependence of the melt apparent viscosity (η_a) on temperatures and the flow activation energy (ΔE_η) was calculated. ΔE_η values for different blends were 64.4(B0), 63.8(B1), 62.6(B3), 61.9(B5) and 61.3(B10) kJ mmol^{-1}, respectively. With increasing ABS-*g*-MAH content, ΔE_η values are slightly decreased, indicating that the blends have smaller dependence of on temperature than that of pure poly(trimethylene terephthalate).

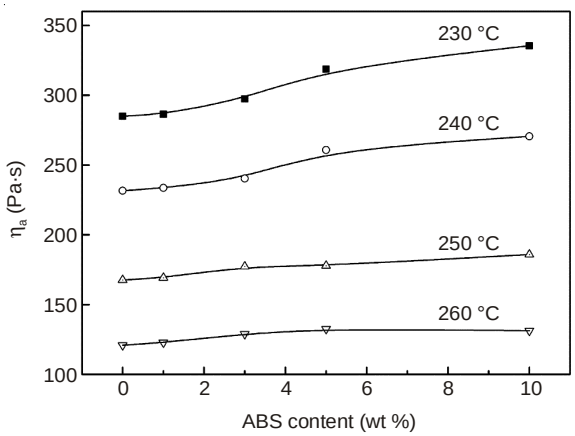

Fig. 9. Relationship between η_a and ABS-*g*-MAH contents at different temperatures

Thermal stability: Fig. 10 shows the TGA results for different blends. A two-stage decomposition of each blend is clearly visible in Fig. 10. The first stage (50-450 °C) is the decomposition of the main chains of poly(trimethylene terephthalate) and ABS-*g*-MAH and the second stage (450-600 °C) is the further decomposition of small molecules. With increasing ABS-*g*-MAH content, the second stage is shifted to higher temperatures because of the polyacrylonitrile in ABS-*g*-MAH which has higher decomposition temperature. The temperature at weight-loss of 5 % ($T_{5\%}$) and the maximum weight-loss rate temperature (T_{max}) are taken as the specific temperature of the degradation process. Apparently, the $T_{5\%}$ and T_{max} of the blends are similar with pure poly(trimethylene terephthalate), which are found to around 388 ± 2 °C for $T_{5\%}$, 417 ± 2 °C for T_{max}. These results indicate that the existence of ABS-*g*-MAH has almost no effect on the thermal stability of the poly(trimethylene terephthalate) and the blends are surely having similar thermal stability.

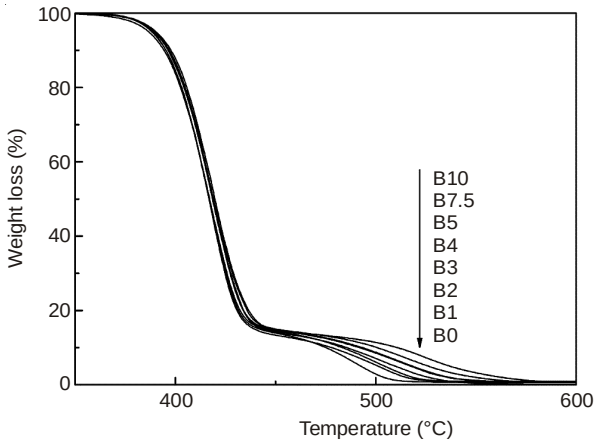

Fig. 10. TGA curves of various poly(trimethylene terephthalate)/ABS-*g*-MAH blends

After thermal aging at 150 °C in atmosphere for various hours, the thermal aging properties were tested and the resulting parameters of B0 and B10 were listed in Table-3. As shown in Table-3, with increasing aging times, the Yid, Wr and ΔE are gradually increased for B0 sample; however, these parameters are greatly increased for B10 sample. This result suggests that the blend with ABS-*g*-MAH component has poor

TABLE-3
THERMAL AGING PARAMETERS OF B0 AND B10

Aging time (h)	B0			B10		
	Yid	Wr	ΔE	Yid	Wr	ΔE
0	8.85	56.29	—	23.52	43.73	—
5	9.50	54.76	0.97	47.72	28.82	9.69
10	13.74	50.08	3.63	50.36	27.13	10.84
20	14.88	45.21	7.04	72.7	18.44	17.75

Yid: yellow index; Wr: white index; E: color difference

thermal aging resistance, which may because of the oxidation behaviors of the double bonds in ABS polymer chain.

Conclusion

In this work, ABS-*g*-MAH was used to toughen poly(trimethylene terephthalate) by melt-blended with poly(trimethylene terephthalate). The results suggest that the blends of poly(trimethylene terephthalate) and ABS-*g*-MAH have apparently improved mechanical properties with about 4-5 % ABS-*g*-MAH content. Poly(trimethylene terephthalate) and ABS-*g*-MAH are compatible. ABS-*g*-MAH can served as nucleating agent to increase the crystallization of poly(trimethylene terephthalate). The addition of ABS-*g*-MAH has little influence on the rheological behavior of the blends. The thermal aging property of the blends is poor because of the easy oxidation of the double bonds in ABS-*g*-MAH molecular chains.

ACKNOWLEDGEMENTS

The work is supported by the financial support from the Natural Science Foundation of Hebei Province (B2010 000219).

REFERENCES

1. J.R. Whinfield and J.T. Dickson, Improvements Relating to the Manufacture of Highly Polymeric Substances, British Patent 578,079 (1941).
2. H.H. Chuah, *Macromolecules*, **34**, 6985 (2001).
3. H.A. Khonakdar, S.H. Jafari and A. Asadinezhad, *Iran Polym. J*., **17**, 19 (2008).
4. D.R. Paul and C.B. Bucknall, Polymer Blends, Wiley, New York (2000).
5. L.A. Utracki, Polymer Blends Handbook, Kluwer Academic, Dordrecht (2003).
6. P. Krutphun and P. Supaphol, *Eur. Polym. J*., **41**, 1561 (2005).
7. M.T. Run, Y.J. Wang, C.G. Yao and J.G. Gao, *Thermochim. Acta*, **447**, 13 (2006).
8. P. Supaphol, N. Dangseeyun and P. Srimoaon, *Polym. Test*., **23**, 175 (2004).
9. P. Supaphol, N. Dangseeyun, P. Thanomkiat and M. Nithitanakul, *J. Polym. Sci., B, Polym. Phys*., **42**, 676 (2004).
10. H.B. Ravikumar, C. Ranganathaiah, G.N. Kumaraswamy and S. Thomas, *Polymer*, **46**, 2372 (2005).
11. I. Aravind, P. Albert, C. Ranganathaiah, J.V. Kurian and S. Thomas, *Polymer*, **45**, 4925 (2004).
12. M.L. Xue, Y.L. Yu, H.H. Chuah, J.M. Rhee, N.H. Kim and J.H. Lee, *Eur. Polym. J*., **43**, 3826 (2007).
13. J.M. Huang, *J. Appl. Polym. Sci*., **88**, 2247 (2003).
14. S.H. Jafari, A. Yavari, A. Asadinezhad, H.A. Khonakdar and F. Böhme, *Polymer*, **46**, 5082 (2005).
15. M.L. Xue, Y.L. Yu, H.H. Chuah and G.X. Qiu, *J. Macromol. Sci. Part B Phys*., **46**, 603 (2007).
16. S.H. Jafari, A. Kalati-vahid, H.A. Khonakdar, A. Asadinezhad, U. Wagenknecht and D. Jehnichen, *Express Polym. Lett*., **6**, 148 (2011).
17. M.T. Run, A.J. Song, Y.J. Wang and C.G. Yao, *J. Appl. Polym. Sci*., **104**, 3459 (2007).
18. M.T. Run, H.Z. Song, Y.J. Wang, C.G. Yao and J.G. Gao, *Front. Chem. Eng. China*, **1**, 238 (2007).
19. M.-L. Xue, Y.-L. Yu, J. Sheng, H. H Chuah and C.-H. Geng, *J. Macromol. Sci. Part B Phys*., **44**, 317 (2005).
20. S. Hashemi, *Express Polym. Lett*., **2**, 474 (2008).
21. E.M. Araújo, E. Hage Jr. and A.J.F. Carvalho, *J. Appl. Polym. Sci*., **87**, 842 (2002).
22. M.L. Xue, Y.L. Yu, H.H. Chuah, J.M. Rhee and J.H. Lee, *J. Appl. Polym. Sci*., **108**, 3334 (2008).
23. O.M. Jazani, A. Arefazar, S.H. Jafari, M.H. Beheshty and A. Ghaemi, *J. Appl. Polym. Sci*., **121**, 2680 (2011).
24. E. Tamaki, A. Hibara, H.B. Kim, M. Tokeshi and T. Kitamori, *J. Chromatogr. A*, **1137**, 256 (2006).
25. J. Sun, G.H. Hu, M. Lambla and H.K. Kotlar, *Polymer*, **37**, 4119 (1996).
26. G.H. Hu and T. Lindt, *J. Polym. Sci. A Polym. Chem*., **31**, 691 (1993).
27. K. Dedecker and G. Groeninckx, *Polymer*, **39**, 4985 (1998).
28. L. Boogh, B. Pettersson and J.A.E. Manson, *Polymer*, **40**, 2249 (1999).
29. R. Mezzenga, L. Boogh and J.A.E. Manson, *Compos. Sci. Technol*., **61**, 787 (2001).
30. J. Fröhlich, H. Kautz, R. Thomann, H. Frey and R. Mülhaupt, *Polymer*, **45**, 2155 (2004).
31. J. Wu, Y.-W. Mai and A.F. Yee, *J. Mater. Sci*., **29**, 4510 (1994).
32. G.M. Kim and G.H. Michler, *Polymer*, **39**, 5699 (1998).
33. Z. Burkus and F. Temelli, *Carbohydr. Polym*., **59**, 459 (2005).